Ionisation efficiencies can be predicted in complicated biological matrices

Analytica Chimica Acta 1032 (2018) 68–74

Contents lists available at ScienceDirect

Analytica Chimica Acta

journal homepage: www.elsevier.com/locate/aca

Ionisation efficiencies can be predicted in complicated biological matrices: A proof of concept

Piia Liigand [a], Jaanus Liigand [a], Filip Cuyckens [b], Rob J. Vreeken [b, c], Anneli Kruve [a, d, *]

[a] Institute of Chemistry, University of Tartu, Ravila 14a, 50411, Tartu, Estonia
[b] Discovery Sciences, Janssen Research and Development, Turnhoutseweg 30, B-2340 Beerse, Belgium
[c] Maastricht Multimodal Molecular Imaging (M4I) Institute, Division of Imaging Mass Spectrometry, Maastricht University, Maastricht, Netherlands
[d] Institut für Chemie und Biochemie, Freie Universität Berlin, Takustraße 3, 14195 Berlin, Germany

HIGHLIGHTS

- 10 compounds were analysed in neat solvent, blood, plasma, urine, cerebrospinal fluid, brain and liver tissue homogenates.
- Assuming equal ionisation efficiencies lead to mismatch of 660 times between actual and predicted ESI/MS responses.
- Ionisation efficiencies were predicted via charged delocalisation and degree of ionisation.
- Ionisation efficiencies allowed reducing prediction mismatch to 8 times.

GRAPHICAL ABSTRACT

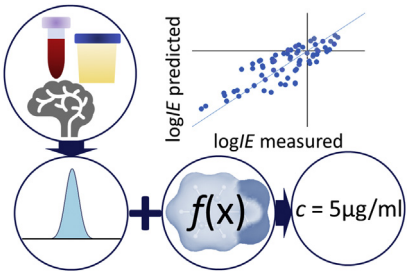

ARTICLE INFO

Article history:
Received 6 April 2018
Received in revised form
18 May 2018
Accepted 29 May 2018
Available online 31 May 2018

Keywords:
Ionisation efficiency
Matrix effect
Non-target
Metabolites

ABSTRACT

The importance of metabolites is assessed based on their abundance. Most of the metabolites are at present identified based on ESI/MS measurements and the relative abundance is assessed from the relative peak areas of these metabolites. Unfortunately, relative intensities can be highly misleading as different compounds ionise with vastly different efficiency in the ESI source and matrix components may cause severe ionisation suppression. In order to reduce this inaccuracy, we propose predicting the ionisation efficiencies of the analytes in seven biological matrices (neat solvent, blood, plasma, urine, cerebrospinal fluid, brain and liver tissue homogenates). We demonstrate, that this approach may lead to an order of magnitude increase in accuracy even in complicated matrices. For the analyses of 10 compounds, mostly drugs, in negative electrospray ionisation mode we reduce the predicted abundance mismatch compared to the actual abundance on average from 660 to 8 times. The ionisation efficiencies were predicted based on i) the charge delocalisation parameter *WAPS* and ii) the degree of ionisation α, and the prediction model was subsequently validated based on the cross-validation method 'leave-one-out'.

1. Introduction

Mass spectrometry (MS) coupled to electrospray ionisation (ESI) is intensively used for the analysis of pharmaceutical drugs in biological matrices [1]. The ability to analyse samples almost

* Corresponding author. Institute of Chemistry, University of Tartu, Ravila 14a, 50411, Tartu, Estonia.
E-mail address: anneli.kruve@ut.ee (A. Kruve).

https://doi.org/10.1016/j.aca.2018.05.072
0003-2670/

directly with direct infusion [2] or flow injection experiments [3] coupled with high-resolution MS has provided a tremendous increase in sample throughput. This technique has proven useful for the analyses of a wide range of samples from human blood plasma [4] to historic wines [5] to ecological samples [6]. For quantitative analysis, nevertheless, standard substances are required due to the large differences in ionisation efficiencies observed in ESI/MS [7–10]. Unfortunately, standard substances are often not available for metabolites and degradation products; therefore, knowing or predicting the ionisation efficiency of these compounds would be extremely useful for estimating their relative importance.

Several research groups have demonstrated that ionisation efficiencies can be correlated with various molecular properties of the compound (pK_a [11,12], log*P* [12,13], surface area [12], charge delocalisation [14,15], gas-phase proton affinity [16,17], etc.). Additionally, our group has shown that measured ionisation efficiencies are transferable from one setup to another [18] and from one solvent system to another [19,20]. Based on these outcomes different models predicting ionisation efficiencies have been developed [10,14,19,21–23]. These models use analytes physicochemical parameters and solvent properties as input parameters. Most commonly used physicochemical parameters are related to the hydrophobicity (log*P*, *WAPS*, *WANS*, C/H ratio) and ionizability of the analyte (pK_a, the degree of ionisation α, etc). We have lately shown [14] that ionisation efficiency can be predicted with high accuracy in ESI negative mode via the degree of charge delocalisation (*WAPS*) and degree of ionisation in solution (α). This approach has been applied for 62 compounds in 10 different solvent systems and serves, therefore, as a good starting point for analysis of complex samples.

In spite of significant research carried out in the field these approaches have remained inapplicable for biological sample analysis. So far, all research groups have predicted ionisation in solvent mixtures without the presence of matrix compounds. However, most analyses are performed in complex matrices. Matrix compounds may significantly decrease or increase the ESI/MS signal of the compound of interest [24,25], this effect is known as matrix effect. The decrease of the signal is much more common and even though the mechanism of ionisation suppression is not completely clear, several trends have been identified. Firstly, matrix effect is expected to arise from the competition of compounds for the surface charge in the ESI droplets [26]. The more hydrophobic the matrix compounds are, the more efficient they are in occupying the droplets' surface and, therefore, these compounds are expected to cause more ionisation suppression [20]. Secondly, the presence of non-volatile solutes causes a severe decrease in ESI/MS response via precipitation of the analyte on the ESI interface [27]. Lastly, gas phase charge transfer from the analyte to matrix components may alter analyte signal [28]. These effects are expected to be even more pronounced for measurements carried out without any or with minimal chromatographic separation [29].

In order to be of practical value for real sample analyses, the ionisation efficiency models should be able to account for the matrix effect. Therefore, it needs to be evaluated whether ionisation efficiency models can also be constructed in matrices relevant for real sample analyses. Based on the previously obtained promising results for ESI negative mode in various solvents we aim to go one step further by predicting the ionisation efficiencies for analysis in biological matrices. Therefore, the aim of this paper is to study whether ionisation efficiencies in ESI negative mode can be predicted in biological matrices (plasma, urine, whole blood, cerebrospinal fluid (CSF), liver and brain tissue homogenates). For this purpose, ionisation efficiency values of 10 compounds, predominantly pharmaceuticals, were measured in different biological matrices with flow injection analyses. The ionisation efficiency model was fitted in each matrix. We use the worst-case scenario, a simple protein precipitation sample preparation without any chromatographic separation of the analyte and matrix compounds, as a proof of concept that ionisation efficiencies can be predicted under severe matrix effect conditions. The method is cross-validated by the 'leave-one-out' validation method.

2. Experimental section

2.1. Compounds and sample pretreatment

Lincomycin hydrochloride (purity ≥95%), dodecanoic acid and fumaric acid (both ≥99%) were obtained from Sigma (Steinheim, Germany) and warfarin (≥99%) from DuPont Pharma (Wilmington, DE, USA). Naproxen (≥98%) was obtained from Synthex Research Center (Edinburgh, UK) and taurocholic acid sodium salt hydrate (≥95%) from Acros Organics (Geel, Belgium). Salicylic acid, benzoic acid and sorbic acid (all ≥99%) were obtained from Reakhim (Moscow, Russia), and 3-[(trifluoromethyl)sulphanyl]benzoic acid (3-CF_3SO_2-benzoic acid, purified by recrystallisation) is a kind gift from prof. L. M. Yagupolskii. Dilution of the samples was performed on pipetting instrument Freedom EVO (TECAN, Switzerland). The structures are shown in Supporting Information.

Liver and brain tissue, urine, and blood from a healthy dog (beagle) were obtained from in-house sources at Janssen Pharmaceutica (Beerse, Belgium), plasma and CSF of a healthy dog (beagle) were obtained from Bioreclamation IVT, USA. For brain and liver tissue, 1 part of tissue was homogenised with 9 parts of MilliQ water to form tissue homogenates. Biological matrices were stored frozen at −20 °C, except for blood which was used fresh (within 2 h). For plasma and blood K_2EDTA was used as anticoagulant. A neat solvent which was a solution of 20/80 0.1% ammonia solution/acetonitrile was used as an example of a simple matrix. Ammonia solution (25% puriss) was obtained from Lach:Ner, Czech Republic and acetonitrile (LC grade) from Merck, Darmstadt, Germany. The mobile phase directed to ESI/MS consisted also of 20/80 0.1% ammonia solution/acetonitrile.

A simple standard protein precipitation sample preparation was carried out: 50 μL of the stock solution of the compound was added to a mixture of 400 μL of acetonitrile and 50 μL of biological matrix (plasma, urine, whole blood, cerebrospinal fluid (CSF), liver or brain tissue (1 part of tissue homogenised with 9 parts of water)). This mixture was thoroughly mixed and centrifuged for 10 min at 13 000 g. The supernatant (injection volume 5 μL) was used for MS analysis. Linear range was 1–200 μM depending on the compound and matrix; the exact concentrations are described in Supporting Information.

2.2. Ionisation efficiency measurements

Ionisation efficiencies were measured in flow injection mode with an Accela liquid chromatograph (Thermo Fisher Scientific, San Jose, USA) coupled with an LTQ ion trap (Thermo-Fisher Scientific, San Jose, USA) mass spectrometer. All measurements were carried out in ESI negative MS scan mode. Sheath gas flow rate 35 psi, auxiliary gas flow 10 a. u., sweep gas flow rate 5 a. u. spray voltage −3.5 kV, and capillary temperature 275 °C were used. The flow rate was 0.2 mL/min.

The measurement of absolute ionisation efficiencies is complicated; therefore, we measured relative ionisation efficiencies (RIE). In order to provide ionisation efficiency values comparable to previous and upcoming studies, all values are provided relative to benzoic acid. The logarithmic ionisation efficiency (log*IE*) of benzoic acid in 20/80 0.1% ammonia solution/acetonitrile has been previously taken as 0 [14].

However, due to severe matrix effect benzoic acid could not be measured in all matrices. Due to high signals even under strong ionisation suppression warfarin was chosen as a within-matrix reference. Thus, all log*RIE* values were first measured relative to warfarin (Fig. 1). The log*RIE* value of each of the compounds was found as the logarithm of the ratios of calibration graph slopes of the compound of interest and warfarin:

$$\log RIE^{compound\ X}_{matrix\ N} = \log \frac{slope^{compound\ X}_{matrix\ N}}{slope^{warfarin}_{matrix\ N}} \quad (1)$$

Then (Fig. 2-B), the log*IE* values in each matrix were attributed to warfarin based on the calibration graph slopes measured in respective matrices. These measurements were performed close in time to avoid drifts in the instrument sensitivity.

$$\log IE^{warfarin}_{matrix\ N} = \log \frac{slope^{warfarin}_{matrix\ N}}{slope^{warfarin}_{solvent}} \quad (2)$$

The log*IE* values for each compound in the specific matrix were, thereafter, found as:

$$\log IE^{compound}_{matrix} = \log RIE^{compound} + \log IE^{warfarin}_{matrix} \quad (3)$$

The anchoring process is in detail described in a video available as Supporting material.

Supplementary video related to this article can be found at https://doi.org/10.1016/j.aca.2018.05.072.

The reproducibility of measurements was calculated as a pooled standard deviation (s).

2.3. COSMO-RS calculations

COSMO-RS method [30] was used for calculating charge delocalisation parameters (*WAPS*/*WANS*) as well as pK_a values. Full geometry optimisation and energy calculation were carried out at the DFT BP TZVP level with the RI approximation and applying the COSMO continuum solvation model for all compounds using Turbomole, ver. 6.4 [31]. The default convergence criteria of Turbomole were used: wavefunction convergence max difference 10^{-6} Hartree, geometry convergence max gradient $|dE/dxyz|$ 10^{-3} Hartree/Bohr. This first computation step yields for every conformer the following data: the geometry of the conformer, detailed data on the shape of molecular cavity, the polarisation charge densities mapped onto the cavity surface, the total electronic energy of the species submerged into a virtual conductor ($\varepsilon = \infty$), and molecular surface area and volume. Molecular cavity refers to the cavity constructed for the particular conformer within the COSMO solvation theory – constructed utilising smoothed spheres using atomic radii ~20% larger than van der Waals radii. This cavity was later used as the molecular volume. The cavity surface refers to the so-called sigma-surface – polarisation charge density on the molecular surface.

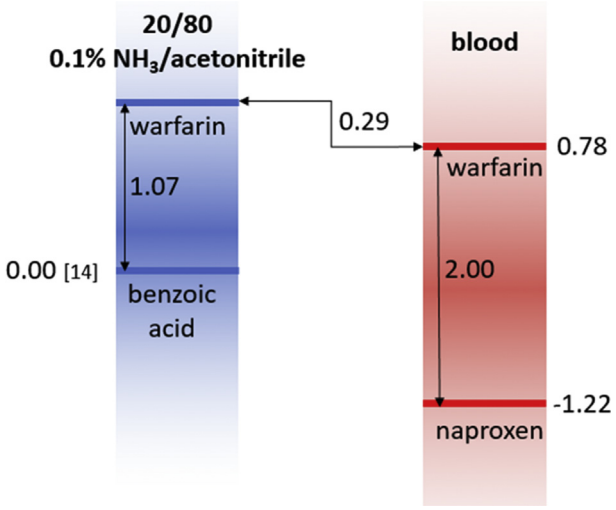

Fig. 1. Anchoring on ionisation efficiencies in different matrices.

Charge delocalisation parameter is calculated as weighted average positive sigma for anions [32]:

$$WAPS = \frac{\int_{\sigma=0}^{\infty} \sigma \cdot p(\sigma) d\sigma}{A \int_{\sigma=0}^{\infty} p(\sigma) d\sigma} \quad (4)$$

Where σ is the polarisation charge density on the surface if anion, $p(\sigma)$ is the probability function of σ and A is the surface area of the anion. The smaller the *WAPS* absolute value, the more delocalised the charge in the anion. It has been proposed that values above 4.5 indicate anions with localised charge [32]. For further information about the COSMO-RS theory, see Ref. [30], for parameters used, see Ref. [33]. The degree of ionisation α of the compounds was calculated from the computed pK_a values and water phase pH (see Table S1)).

2.4. Model development and validation

Based on the calculated physiochemical parameters and measured log*IE* values a predictive model was fit in each matrix. Multilinear regression analysis was used to obtain the model describing the relationship between log*IE* and physicochemical properties. The general form of the equation was:

$$\log IE = coef_{WAPS} \cdot WAPS + coef_{\alpha} \cdot \alpha + intercept, \quad (5)$$

where the coefficients depend on the matrix.

For each model root-mean-square error (s_{RMSE}) was found to describe the differences between predicted log*IE* values and measured values [34].

$$s_{RMSE} = \sqrt{\left(\log IE_{predicted} - \log IE_{experimental}\right)^2} \quad (6)$$

Additionally, the goodness-of-fit test was used to estimate the quality of the developed matrices.

$$F = \frac{\sum \left(\log IE_{predicted} - \overline{\log IE_{experimental}}\right)^2 \Big/ (n-1)}{\sum \left(\log IE_{experimental} - \log IE_{predicted}\right)^2 \Big/ (r-n)} \quad (7)$$

Where n is the number of compounds and r is the number of concentration levels incorporated into the calibration graph and $\overline{\log IE_{experimental}}$ denotes the mean value of all the measured log*IE* values. From F-values the p-values were calculated using the degrees of freedom of the numerator and denominator. Higher p-values indicate higher explained variation in log*IE* values by the model.

In order to validate the obtained results, we used the cross-validation method 'leave-one-out' (LOO) approach. Cross-validation was preferred due to the need to estimate the applicability of the method over a wide range of log*IE* values. LOO

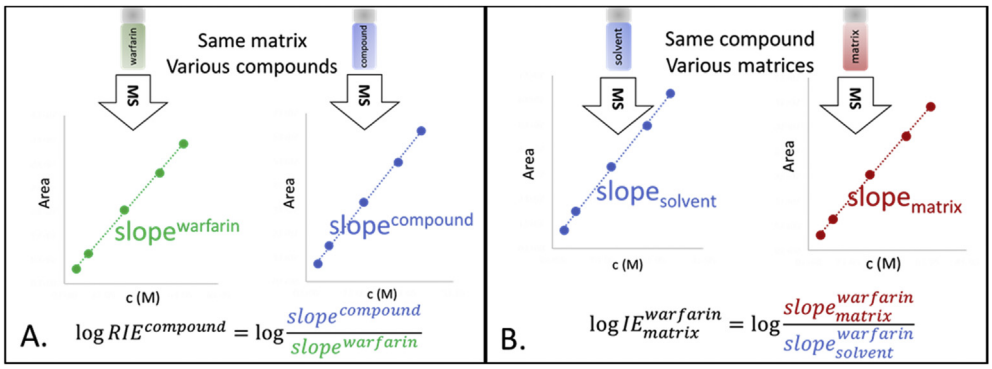

Fig. 2. Measurement procedure (A) to obtain log*RIE* values for analytes relative to warfarin in one matrix; (B) to obtain log*IE* values for warfarin in different matrixes relative to warfarin in neat solvent.

approach means that each compound was left out from the model fitting process once; thereafter, the model was used to predict the log*IE* value of the compound not involved in the model development. After this, the process was repeated for another compound, so that each compound was left out once from the model development. In case of conventional validation set approach, the log*IE* values could have been predicted only for ca 2 to 3 compounds, which would provide insufficient information about the model.

3. Results and discussion

The span of the log*IE* values (Table 1) measured within one biological matrix varied from 2.40 log*IE* units in the brain to 4.47 log*IE* units in blood. The narrowest span was observed in the neat solvent (ca 1.67 log*IE* units). The difference in spans demonstrates the extent of compressing or expanding the log*IE* scales by the matrix compounds.

The variation of log*IE* values of compounds between different matrices was significant: from 0.98 (warfarin, $\log IE_{solv} - \log IE_{urine}$, 1.07−0.09) to 3.09 (fumaric acid, $\log IE_{solv} - \log IE_{blood}$, −0.60 − (−3.69)) log*IE* units. This variation demonstrates that ionisation efficiencies are considerably influenced by the matrix components. For example, in blood samples the signal of warfarin is supressed by 89.5% relative to neat solvent. Additionally, we observed that the variation in log*IE* values from one matrix to another was lower for compounds with higher ionisation efficiencies (e.g. warfarin and taurocholic acid versus fumaric acid and sorbic acid).

In the literature, it has been shown that matrix effect may vary with analyte concentration [35,36]. The concentration dependence of matrix effect is a very delicate question and it may depend on the way matrix effect is calculated. Namely, differences are observed if calibration graph slopes or peak areas are used [35]. This is especially important if matrix alters the linear range of the method or intercept values [37,38]. Here all measurements are done in the linear range and calibration graph slopes are used to calculate matrix effect. If the measurements are in the linear range, it does not matter which specific concentration are used, as calculated slope is independent of the concentrations in this range.

The order of the log*IE* values of the compounds remained roughly the same from one matrix to another. This means that compounds with higher log*IE* values in the neat solvent are also ionised better in the presence of matrix components. The same was confirmed by the correlation studies (see Supporting Information). The log*IE* values in different biological matrices were in good correlation with the log*IE* values in the neat solvent (20/80 0.1% ammonia solution/acetonitrile); see Table 1. The highest correlation was observed between log*IE* values measured in urine and brain tissue homogenate with log*IE* values measured in the neat solvent ($R^2 = 0.87$ for both). The lowest correlation was observed between log*IE* values measured in CSF extract and log*IE* values measured in the neat solvent ($R^2 = 0.67$). The correlation graphs are presented in SI. Additionally, the IE values measured in the neat solvent are in good correlation with previous measurements [19] carried out on a different instrument ($R^2 = 0.95$).

For all correlations, the intercept values were negative; this pinpoints that biological matrices suppress ionisation for the

Table 1
The ionisation efficiencies (log*IE*) measured in various matrices and neat solvent ($\log IE_{solv}$) together with physicochemical parameters calculated with COSMO-RS. $\log IE^{*}_{solv}$ values refer to the ionisation efficiency values from Ref. [19] that have been measured on a different instrument and in 20/80 0.1% ammonia/acetonitrile mobile phase. The reproducibility of measurements was calculated as a pooled standard deviation – *s*. NA[a] – values not possible to measure; NA[b] – compounds not measured before in the same solvent.

	$\log IE_{urine}$	$\log IE_{plasma}$	$\log IE_{blood}$	$\log IE_{CSF}$	$\log IE_{liver}$	$\log IE_{brain}$	$\log IE_{solv}$	$\log IE^{*}_{solv}$	pK_a	α	$WAPS \cdot 10^5$
warfarin	0.09	0.68	0.78	0.34	0.62	0.94	1.07	NA[b]	4.63	1.00	2.43
taurocholic acid	−0.25	−0.16	−0.29	−0.31	0.29	0.54	0.97	NA[b]	−2.36	1.00	1.92
3-CF_3SO_2-benzoic acid	−0.42	0.33	0.06	−0.28	0.22	0.38	0.83	1.69	3.77	1.00	3.65
salicylic acid	−0.76	−0.42	−0.42	−0.68	−0.38	−0.28	0.34	0.39	3.33	1.00	6.06
dodecanoic acid	−1.55	−1.10	−0.82	−0.58	−0.57	−0.41	0.24	NA[b]	4.96	1.00	2.85
benzoic acid	−2.09	−2.55	−2.90	NA[a]	−1.58	−1.17	0.00	0.00	4.63	1.00	7.07
naproxen	−2.28	−1.62	−1.22	−1.67	−0.69	−0.66	0.12	NA[b]	5.10	1.00	3.46
lincomycin	−2.38	−1.55	−1.90	−1.90	−1.20	−1.14	0.20	NA[b]	11.65	0.11	2.17
sorbic acid	−2.43	−1.50	−1.25	−0.93	−1.06	−0.87	−0.36	−0.40	5.38	1.00	7.01
fumaric acid	−2.80	−3.53	−3.69	−2.88	−1.84	−1.46	−0.60	NA[b]	3.68	1.00	8.78
s	0.33	0.15	0.25	0.14	0.10	0.19	0.12				
R^2 with neat solvent	0.87	0.82	0.71	0.67	0.86	1.37	–	0.95			
Slope	1.80	2.15	2.10	1.42	1.40	1.37	–	1.75			
Intercept	−2.00	−1.74	−1.75	−1.50	−1.01	−0.80	–	0.07			

studied compounds. For all biological matrices, the correlation graph slopes were significantly above 1. These two findings show that in general the signal of compounds with lower ionisation efficiencies is suppressed more than the signal of compounds with higher ionisation efficiencies. This is well in line with the surface excess charge model proposed by C.G. Enke [26]. According to this model, the ionisation efficiency of a compound depends both on the compounds affinity towards droplet surface charge and on the co-eluting compounds affinity towards droplets surface charge. Compounds with lower affinity have lower ionisation efficiencies, and additionally, are more easily outcompeted from the surface of the droplets by the matrix compounds.

Based on the correlation graphs the most complicated matrices were blood, plasma and urine. For these matrices, the intercepts were the lowest and slopes the highest. Blood and plasma are known to cause severe ionisation suppression even after protein precipitation due to the omnipresence of phospholipids [39]. Additionally, urine samples are known to have a high salt concentration which is not completely removed by the sample preparation. For example, Dams et al. have observed ionisation suppression of 85% even after using protein precipitation with acetonitrile as a sample preparation method [40]. High salt concentrations are known to cause severe ionisation suppression [41] due to analyte precipitation in ESI [27].

A good correlation between log*IE* values measured in matrices and in the neat solvent hints that ionisation efficiencies can be predicted in the matrices similarly to the already published predictions in the neat solvent [10,14,15]. In order to test this further, different physicochemical parameters were used for modelling. Previously [14,15,19], we have shown that log*IE* values in the neat solvent are best described by charge delocalisation parameter *WAPS* and degree of ionisation α. In this study, the *WAPS* values also had the highest correlation with log*IE* values measured in biological matrices. These parameters were also used to fit the multilinear models for predicting the log*IE* values measured in biological matrices. The obtained models have the general form as Eq. (5) and the respective constants are described in Table 2. The obtained models possess good predictive power; the R^2 values ranged from 0.55 (urine) to 0.81 (liver). The obtained fits are graphically shown in Fig. 3 (each colour represents one matrix).

The coefficients for *WAPS* in the model fitted for log*IE* values in urine, liver, blood and brain matrix are very similar and only in urine matrix, the intercept value became statistically significant. This can most likely be attributed to the relatively high salt content in urine as compared to the other matrices. Obviously, the salts have a much larger effect on the ion suppression than either the lipids, bile acids or proteins remaining after sample preparation in other matrices.

The accuracy of the models can also be described with the root mean square error of the models from the LOO validation, $s_{RMSE} = 0.86$ log*IE* units. This value shows that on average the mismatch between the predicted and measured ionisation efficiencies is lower than 8.3 times. Until now, in the absence of authentic standards, equal ionisation efficiencies are assumed in all matrices. For example, if the ionisation efficiencies for all compounds used in this study are assumed to be equal to the ionisation efficiency of benzoic acid and peak areas are used to describe the abundance of the compounds present in the sample it would lead to an average error of 660 times. This means, that the proposed approach improves predicting ionisation efficiency by almost two orders of magnitude.

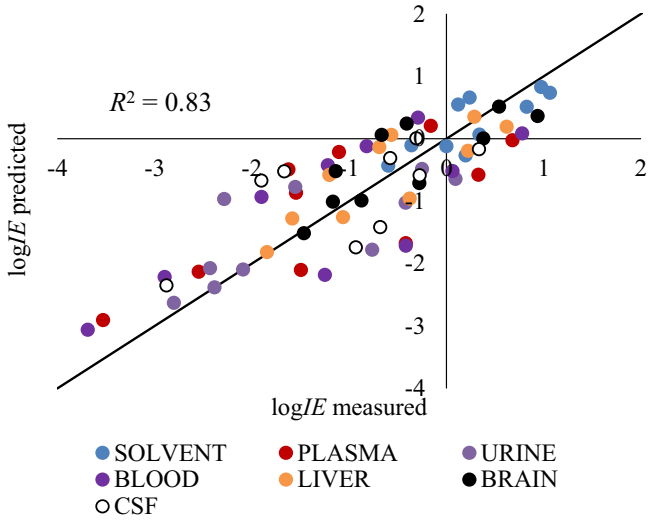

Fig. 3. Correlation of all the measured log*IE* values and predicted log*IE* values in different matrices. Each dot represents one compound in one matrix, different colours indicate different matrices. (For interpretation of the references to colour in this figure legend, the reader is referred to the Web version of this article.)

Moreover, all experiments in this study were carried out in flow injection mode without any chromatographic separation. Therefore, the ionisation efficiencies of all of the studied compounds are affected by all of the matrix compounds present after sample preparation. In case of chromatographic separation, all of the analysed compounds would co-elute only with a fraction of matrix compounds and it is commonly expected that the matrix effect would significantly decrease. Nevertheless, each analyte would co-elute with different matrix compounds and, therefore, much more complicated effect on the ionisation efficiencies could occur. This could result in a lower correlation between log*IE* values measured in the neat solvent and measured in matrices. However, much lower ionisation suppression is expected. Additionally, differences arising from chromatographic separation could be accounted for by adding the calibration compounds via post-column infusion techniques [42,43] and developing the predictive model coefficients (Eq. (5)) based on the signals of these post-column infused compounds. The results obtained with flow injection analyses serve as a good starting point for developing a universal approach that would be compatible both with liquid chromatography and flow injection

Table 2
Coefficients for predicting log*IE* values in different matrices. The general form of the equation is $\log IE = coef_{WAPS} \cdot WAPS + coef_{\alpha} \cdot \alpha + intercept$.

	$coef_{WAPS}$			$coef_{\alpha}$			intercept			R^2	s_{RMSE}	s_{RMSE} from LOO validation	p Goodness-of-Fit
Solvent	−0.18	±	0.05	1.18	±	0.26				0.72	0.35	0.36	0.997
Urine	−0.31	±	0.12	2.04	±	1.01	−1.93	±	0.93	0.55	0.80	0.83	0.988
Plasma	−0.45	±	0.13	1.08	±	0.68				0.77	0.90	1.02	0.993
Blood	−0.50	±	0.13	1.29	±	0.69				0.78	0.91	1.31	0.996
Liver	−0.32	±	0.07	0.96	±	0.37				0.81	0.49	0.82	0.999
Brain	−0.30	±	0.07	1.08	±	0.38				0.73	0.50	0.52	0.997
CSF	−0.34	±	0.12	0.66	±	0.63				0.71	0.83	1.19	0.977

metabolomics. Additionally, as the push towards high throughput is ever increasing and this is driving metabolomics studies also towards flow injection analyses [3,44], the current approach already is applicable.

4. Conclusions

We have presented an accurate approach to predict ionisation efficiencies in ESI negative mode for complex biological matrices, namely in blood, plasma, CSF as well as in brain and liver tissue homogenates. Based on the validation, the average predicting power was estimated to be 0.86 log*IE* units (8.3 times mismatch between measured and predicted ionisation efficiencies). This accuracy is sufficient to allow a significantly improved estimation of the relative abundance of analytes when reference standards are lacking or not used. In the future, we would like to evaluate and expand the approach for the studied matrices in the positive ESI mode and for analyses with LC separation.

Author contributions

P.L. and J.L. performed ionisation efficiency measurements P.L. wrote main part of the text, J.L., F.C., R.J.V and A.K. helped with preparing the manuscript. All authors have given approval to the final version of the manuscript.

Notes

The authors declare no competing financial interest.

Acknowledgement

This work was supported by Personal Research Funding Project 34 from the Estonian Research Council, by smart specialisation doctoral stipend and by Erasmus + stipend. The authors would like to thank Janssen Pharmaceutica NV (Beerse, Belgium) where this study was carried out.

Appendix A. Supplementary data

Supplementary data related to this article can be found at https://doi.org/10.1016/j.aca.2018.05.072.

References

[1] A. Doerr, J. Finkelstein, I. Jarchum, C. Goodman, B. Dekker, The nature milestones in mass spectrometry, Br. J. Pharmacol. 12 (2015) S1–S45.
[2] M.A. García-Sevillano, T. García-Barrera, F. Navarro, Z. Montero-Lobato, J.L. Gómez-Ariza, Shotgun metabolomic approach based on mass spectrometry for hepatic mitochondria of mice under arsenic exposure, Biometals 28 (2015) 341–351, https://doi.org/10.1007/s10534-015-9837-9.
[3] T. Fuhrer, N. Zamboni, High-throughput discovery metabolomics, Curr. Opin. Biotechnol. 31 (2015) 73–78, https://doi.org/10.1016/j.copbio.2014.08.006.
[4] K. Schuhmann, R. Almeida, M. Baumert, R. Herzog, S.R. Bornstein, A. Shevchenko, Shotgun lipidomics on a LTQ Orbitrap mass spectrometer by successive switching between acquisition polarity modes: shotgun lipidomics with polarity switching, J. Mass Spectrom. 47 (2012) 96–104, https://doi.org/10.1002/jms.2031.
[5] P. Jeandet, S.S. Heinzmann, C. Roullier-Gall, C. Cilindre, A. Aron, M.A. Deville, F. Moritz, T. Karbowiak, D. Demarville, C. Brun, F. Moreau, B. Michalke, G. Liger-Belair, M. Witting, M. Lucio, D. Steyer, R.D. Gougeon, P. Schmitt-Kopplin, Chemical messages in 170-year-old champagne bottles from the Baltic Sea: revealing tastes from the past, Proc. Natl. Acad. Sci. Unit. States Am. 112 (2015) 5893–5898, https://doi.org/10.1073/pnas.1500783112.
[6] Norbert Hertkorn, Mourad Harir, Kaelin M. Cawley, Philippe Schmitt-Kopplin, Rudolf Jaffé, Molecular characterization of dissolved organic matter from subtropical wetlands: a comparative study through the analysis of optical properties, NMR and FTICR/MS, Biogeosciences 13 (2016) 2257–2277, https://doi.org/10.5194/bg-13-2257-2016.
[7] L. Tang, P. Kebarle, Dependence of ion intensity in electrospray mass spectrometry on the concentration of the analytes in the electrosprayed solution, Anal. Chem. 65 (1993) 3654–3668.
[8] N.B. Cech, C.G. Enke, Relating electrospray ionization response to nonpolar character of small peptides, Anal. Chem. 72 (2000) 2717–2723, https://doi.org/10.1021/ac9914869.
[9] S. Zhou, K.D. Cook, A mechanistic study of electrospray mass spectrometry: charge gradients within electrospray droplets and their influence on ion response, J. Am. Soc. Mass Spectrom. 12 (2001) 206–214, https://doi.org/10.1016/S1044-0305(00)00213-0.
[10] M. Oss, A. Kruve, K. Herodes, I. Leito, Electrospray ionization efficiency scale of organic compounds, Anal. Chem. 82 (2010) 2865–2872, https://doi.org/10.1021/ac902856t.
[11] V.J. Mandra, M.G. Kouskoura, C.K. Markopoulou, Using the partial least squares method to model the electrospray ionization response produced by small pharmaceutical molecules in positive mode: modelling positive electrospray ionization response, Rapid Commun. Mass Spectrom. 29 (2015) 1661–1675, https://doi.org/10.1002/rcm.7263.
[12] J. Golubović, C. Birkemeyer, A. Protić, B. Otašević, M. Zečević, Structure–response relationship in electrospray ionization-mass spectrometry of sartans by artificial neural networks, J. Chromatogr. A 1438 (2016) 123–132, https://doi.org/10.1016/j.chroma.2016.02.021.
[13] T. Henriksen, R.K. Juhler, B. Svensmark, N.B. Cech, The relative influences of acidity and polarity on responsiveness of small organic molecules to analysis with negative ion electrospray ionization mass spectrometry (ESI-MS), J. Am. Soc. Mass Spectrom. 16 (2005) 446–455, https://doi.org/10.1016/j.jasms.2004.11.021.
[14] A. Kruve, K. Kaupmees, J. Liigand, I. Leito, Negative electrospray ionization via deprotonation: predicting the ionization efficiency, Anal. Chem. 86 (2014) 4822–4830, https://doi.org/10.1021/ac404066v.
[15] P. Liigand, K. Kaupmees, K. Haav, J. Liigand, I. Leito, M. Girod, R. Antoine, A. Kruve, Think negative: finding the best electrospray ionization/MS mode for your analyte, Anal. Chem. 89 (2017) 5665–5668, https://doi.org/10.1021/acs.analchem.7b00096.
[16] M.H. Amad, N.B. Cech, G.S. Jackson, C.G. Enke, Importance of gas-phase proton affinities in determining the electrospray ionization response for analytes and solvents, J. Mass Spectrom. 35 (2000) 784–789.
[17] C.M. Alymatiri, M.G. Kouskoura, C.K. Markopoulou, Decoding the signal response of steroids in electrospray ionization mode (ESI-MS), Anal. Methods 7 (2015) 10433–10444, https://doi.org/10.1039/C5AY02839F.
[18] J. Liigand, A. Kruve, P. Liigand, A. Laaniste, M. Girod, R. Antoine, I. Leito, Transferability of the electrospray ionization efficiency scale between different instruments, J. Am. Soc. Mass Spectrom. 26 (2015) 1923–1930, https://doi.org/10.1007/s13361-015-1219-6.
[19] A. Kruve, K. Kaupmees, Predicting ESI/MS signal change for anions in different solvents, Anal. Chem. 89 (2017) 5079–5086, https://doi.org/10.1021/acs.analchem.7b00595.
[20] A. Kruve, Influence of mobile phase, source parameters and source type on electrospray ionization efficiency in negative ion mode: influence of mobile phase in ESI/MS, J. Mass Spectrom. 51 (2016) 596–601, https://doi.org/10.1002/jms.3790.
[21] K.R. Chalcraft, R. Lee, C. Mills, P. Britz-McKibbin, Virtual quantification of metabolites by capillary electrophoresis-electrospray ionization-mass spectrometry: predicting ionization efficiency without chemical standards, Anal. Chem. 81 (2009) 2506–2515, https://doi.org/10.1021/ac802272u.
[22] T.B. Nguyen, S.A. Nizkorodov, A. Laskin, J. Laskin, An approach toward quantification of organic compounds in complex environmental samples using high-resolution electrospray ionization mass spectrometry, Anal Methods 5 (2013) 72–80, https://doi.org/10.1039/C2AY25682G.
[23] L. Wu, Y. Wu, H. Shen, P. Gong, L. Cao, G. Wang, H. Hao, Quantitative structure–ion intensity relationship strategy to the prediction of absolute levels without authentic standards, Anal. Chim. Acta 794 (2013) 67–75, https://doi.org/10.1016/j.aca.2013.07.034.
[24] P.J. Taylor, Matrix effects: the Achilles heel of quantitative high-performance liquid chromatography–electrospray–tandem mass spectrometry, Clin. Biochem. 38 (2005) 328–334, https://doi.org/10.1016/j.clinbiochem.2004.11.007.
[25] A. Kruve, A. Künnapas, K. Herodes, I. Leito, Matrix effects in pesticide multi-residue analysis by liquid chromatography–mass spectrometry, J. Chromatogr. A 1187 (2008) 58–66, https://doi.org/10.1016/j.chroma.2008.01.077.
[26] C.G. Enke, A predictive model for matrix and analyte effects in electrospray ionization of singly-charged ionic analytes, Anal. Chem. 69 (1997) 4885–4893, https://doi.org/10.1021/ac970095w.
[27] R. King, R. Bonfiglio, C. Fernandez-Metzler, C. Miller-Stein, T. Olah, Mechanistic investigation of ionization suppression in electrospray ionization, J. Am. Soc. Mass Spectrom. 11 (2000) 942–950, https://doi.org/10.1016/S1044-0305(00)00163-X.
[28] J. Zrostlıková, J. Hajšlová, J. Poustka, P. Begany, Alternative calibration approaches to compensate the effect of co-extracted matrix components in liquid chromatography–electrospray ionisation tandem mass spectrometry analysis of pesticide residues in plant materials, J. Chromatogr. a. 973 (n.d.) 13–26. doi:10.1016/S0021-9673(02)01196-2.
[29] W.M.A. Niessen, P. Manini, R. Andreoli, Matrix effects in quantitative pesticide analysis using liquid chromatography–mass spectrometry, Mass Spectrom. Rev. 25 (2006) 881–899, https://doi.org/10.1002/mas.20097.
[30] A. Klamt, COSMO-rs from Quantum Chemistry to Fluid Phase Thermodynamics and Drug Design, Elsevier Science Ltd, Amsterdam, 2005.

[31] TURBOMOLE V6.4, A development of university of karlsruhe and forschungszentrum karlsruhe GmbH, 1989-2007, TURBOMOLE GmbH, since 2007, available from, http://www.turbomole.com, 2012.
[32] K. Kaupmees, I. Kaljurand, I. Leito, Influence of water content on the acidities in acetonitrile. Quantifying charge delocalization in anions, J. Phys. Chem. 114 (2010) 11788–11793, https://doi.org/10.1021/jp105670t.
[33] P. Liigand, K. Kaupmees, A. Kruve, Ionization efficiency of doubly charged ions formed from polyprotic acids in electrospray negative mode, J. Am. Soc. Mass Spectrom. 27 (2016) 1211–1218, https://doi.org/10.1007/s13361-016-1384-2.
[34] J.N. Miller, J.C. Miller, Statistics and Chemometrics for Analytical Chemistry, 6. ed, Prentice Hall, Harlow, 2010.
[35] A. Kruve, R. Auling, K. Herodes, I. Leito, Study of liquid chromatography/electrospray ionization mass spectrometry matrix effect on the example of glyphosate analysis from cereals: matrix effect on the example of glyphosate analysis, Rapid Commun. Mass Spectrom. 25 (2011) 3252–3258, https://doi.org/10.1002/rcm.5222.
[36] A. Furey, M. Moriarty, V. Bane, B. Kinsella, M. Lehane, Ion suppression; A critical review on causes, evaluation, prevention and applications, Talanta 115 (2013) 104–122, https://doi.org/10.1016/j.talanta.2013.03.048.
[37] P. Manini, R. Andreoli, A. Mutti, Application of liquid chromatography–mass spectrometry to biomonitoring of exposure to industrial chemicals, Toxicol. Lett. 162 (2006) 202–210, https://doi.org/10.1016/j.toxlet.2005.09.023.
[38] M. Villagrasa, M. Guillamón, E. Eljarrat, D. Barceló, Matrix effect in liquid chromatography–electrospray ionization mass spectrometry analysis of benzoxazinoid derivatives in plant material, J. Chromatogr. A 1157 (2007) 108–114, https://doi.org/10.1016/j.chroma.2007.04.040.
[39] J. Little, M. Wempe, C. Buchanan, Liquid chromatography–mass spectrometry/mass spectrometry method development for drug metabolism studies: examining lipid matrix ionization effects in plasma, J. Chromatogr. B 833 (2006) 219–230, https://doi.org/10.1016/j.jchromb.2006.02.011.
[40] R. Dams, M.A. Huestis, W.E. Lambert, C.M. Murphy, Matrix effect in bio-analysis of illicit drugs with LC-MS/MS: influence of ionization type, sample preparation, and biofluid, J. Am. Soc. Mass Spectrom. 14 (2003) 1290–1294, https://doi.org/10.1016/S1044-0305(03)00574-9.
[41] K. Lanckmans, A. Van Eeckhaut, S. Sarre, I. Smolders, Y. Michotte, Capillary and nano-liquid chromatography–tandem mass spectrometry for the quantification of small molecules in microdialysis samples: comparison with microbore dimensions, J. Chromatogr. A 1131 (2006) 166–175, https://doi.org/10.1016/j.chroma.2006.07.090.
[42] O. González, M. van Vliet, C.W.N. Damen, F.M. van der Kloet, R.J. Vreeken, T. Hankemeier, Matrix effect compensation in small-molecule profiling for an LC–TOF platform using multicomponent postcolumn infusion, Anal. Chem. 87 (2015) 5921–5929, https://doi.org/10.1021/ac504268y.
[43] J. Rossmann, L.D. Renner, R. Oertel, A. El-Armouche, Post-column infusion of internal standard quantification for liquid chromatography-electrospray ionization-tandem mass spectrometry analysis – pharmaceuticals in urine as example approach, J. Chromatogr. A 1535 (2018) 80–87, https://doi.org/10.1016/j.chroma.2018.01.001.
[44] M. Zampieri, K. Sekar, N. Zamboni, U. Sauer, Frontiers of high-throughput metabolomics, Curr. Opin. Chem. Biol. 36 (2017) 15–23, https://doi.org/10.1016/j.cbpa.2016.12.006.